CHEMISTRY
A EUROPEAN JOURNAL

DOI: 10.1002/chem.200901514

A New Highly Selective and Sensitive Assay for Fluorescence Imaging of ·OH in Living Cells: Effectively Avoiding the Interference of Peroxynitrite

Ping Li, Ting Xie, Xia Duan, Fabiao Yu, Xu Wang, and Bo Tang*[a]

Abstract: A new nonredox fluorescent probe to realize the imaging of hydroxyl radicals (·OH) in living cells was designed and synthesized. The structure comprised the fluorescent dye boron dipyrromethene (BDP) and a 2,2,6,6-tetramethyl-1-piperidinoxyl (TEMPO) unit. This probe could rapidly respond to ·OH with a detection limit of 18 pM, and it possessed superior photostability and pH insensitivity. Other reactive oxygen species (ROS) and relevant intracellular components did not interfere. In particular, the important problem of $ONOO^-$ interference was efficiently avoided. An MTT assay proved that the probe was not very cytotoxic. The probe could penetrate into intact cell membranes to selectively detect intracellular ·OH without causing cellular damage in living mice macrophages, normal human liver cells. and human hepatoma cells. These advantageous characteristics make the fluorescent probe potentially useful as a new candidate to detect ·OH in broad biosystems.

Keywords: dyes/pigments · fluorescent probes · radicals

Introduction

Reactive oxygen species (ROS), such as superoxide ($O_2^{-\bullet}$), hydrogen peroxide (H_2O_2), hydroxyl radicals (·OH), nitric oxide (NO), and peroxynitrite ($ONOO^-$), are generated in the course of biological metabolism. Many physiological and pathological conditions are associated with the accumulation of ROS, including carcinogenesis,[1] inflammation,[2] ischemia-reperfusion injury,[3] and eukaryotic signal transduction.[4–6] In particular, there is considerable evidence that ·OH can damage DNA bases[1] and mediate redox alteration of cell-membrane Ca^{2+} channels.[7] In order to fully understand the biological roles of ·OH, a major focus of research is to exploit highly selective and sensitive methods to monitor the concentration of hydroxyl radicals in biosystems in real time and real space. Among these methods, spectrofluorimetry is powerful due to its high sensitivity, simplicity in data collection, and high spatial resolution in imaging techniques.[8,9]

In recent years, there have been some research efforts toward the development of fluorescence techniques for detecting ·OH. Existing fluorescence methods encounter some problems in biosystems. Although a variety of fluorescent probes requiring excitation wavelengths in the UV region have successfully been used to detect ·OH,[10–12] cell damage and background fluorescence restrict their practical application in biosystems. Furthermore, other probes with visible-region excitation have been reported.[13–18] However, their fluorescence signals suffer from interference by other ROS, including $O_2^{-\bullet}$,[19] peroxyl, alkoxyl, and carbonate ($CO_3^{\bullet-}$) species.[13–17] In particular, interference from $ONOO^-$[13–17,20] is a severe obstacle in detecting ·OH because of the similarity between $ONOO^-$ and ·OH with regard to their strong oxidation capacity. In addition, some fluorescent probes need a long time for the analysis process,[21,22] are liable to photobleach,[13–17] or are highly sensitive to pH variation.[23] Moreover, the sensitivities of the current methods make it difficult to break through the nanomol level.[10–12]

It is well known that ·OH is a very reactive species that has a lifetime of about two nanoseconds in aqueous solution. Furthermore, the concentration of ·OH is low in biological systems. Clearly, there is a strong need and interest in developing highly selective and sensitive fluorescent probes to monitor ·OH in biological samples. Up to now, no perfect probe could realize the fluorescence imaging of ·OH in living cells, except our group's Au nanoparticles–DNA–fluorescein (FAM) probe.[24] However, this probe suffers

[a] Dr. P. Li, T. Xie, X. Duan, F. Yu, Dr. X. Wang, Prof. Dr. B. Tang
College of Chemistry, Chemical Engineering and Materials Science
Shandong Normal University, Jinan, 250014 (P. R. China)
Fax: (+86) 531-86186033
E-mail: tangb@sdnu.edu.cn

Supporting information for this article is available on the WWW under http://dx.doi.org/10.1002/chem.200901514.

from high requirements during the synthesis process because of the complexity of the two-end modification of DNA. Therefore, our overall strategy was to develop an ideal fluorescent probe to visualize intracellular ·OH. First, we planned to improve the reaction rate and selectivity of the probe. A 4-hydroxy-2,2,6,6-tetramethyl-1-piperidinoxyl (4-hydroxy-TEMPO) unit was introduced (Scheme 1) because

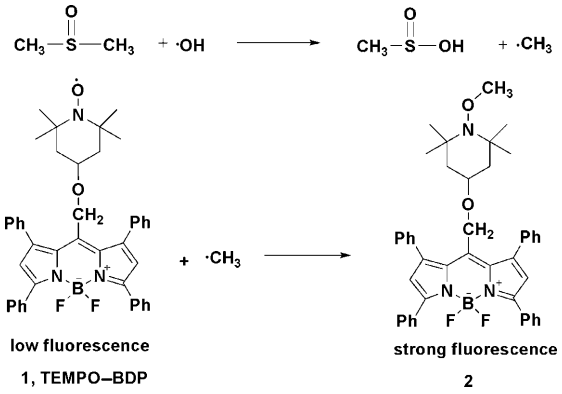

Scheme 1. Mechanism of the reaction.

the nitroxide of TEMPO rapidly reacts with a methyl radical to produce a stable *O*-methoxy group;[25] the ·CH_3 species is formed by a quantitative reaction between ·OH and dimethylsulfoxide (DMSO).[26] Therefore, we assumed that the probe would show good selectivity due to the above-mentioned nonredox mechanism. Second, we employed a boron dipyrromethene (BDP) dye to realize the high sensitivity. This type of fluorophore has exhibited desirable spectral characteristics in terms of a high absorption coefficient and fluorescence quantum yield. In addition, this probe containing BDP should be highly photostable and less sensitive to the pH value and oxidative compounds.[27,28] Third, excitation could be achieved at rather long wavelengths (about 560 nm) to effectively minimize cell damage and avoid endogenous fluorescence from coexisting biomolecules.

Based on these thoughts and by covalently combining BDP with TEMPO, we designed a new fluorescent probe, TEMPO–BDP (**1**), with high selectivity and sensitivity (Scheme 1). The probe itself was not very fluorescent because the fluorescence of BDP was quenched effectively by intramolecular electron exchange between BDP and TEMPO.[29,30] The nitroxide moiety of this probe reacted rapidly with ·CH_3 to produce the diamagnetic compound quantitatively, which resulted in the restoration of BDP fluorescence (Scheme 1). In this paper, the spectral characteristics of the probe were investigated under a simulated physiological environment, and the sensitivity and selectivity of the method toward ·OH were evaluated. Finally, the probe was applied to the imaging of ·OH in mice macrophages (RAW264.7), normal human liver cells (HL7702), and human hepatoma cells (HepG2).

Results and Discussion

Spectral properties: The spectral characteristics of TEMPO–BDP were tested by its reaction with hydroxyl radicals in 2-[4-(2-hydroxyethyl)-1-piperazinyl]ethanesulfonic acid (HEPES) buffer. Figure 1 shows that the λ_{max} values of excitation (lines 1 and 3) and emission (lines 2 and 4) of TEMPO–BDP lie at 560 and 601 nm, respectively. The fluorescence quantum yields of TEMPO–BDP and the fluorescent product were 0.03 and 0.20, respectively, when the TEMPO–BDP (2.0 μM) reacted with various concentrations of ·CH_3 formed quantitatively from the reaction between ·OH and DMSO. (DMSO is exceedingly nontoxic and can be tolerated by living systems in concentrations of up to 1 M.[31–36])

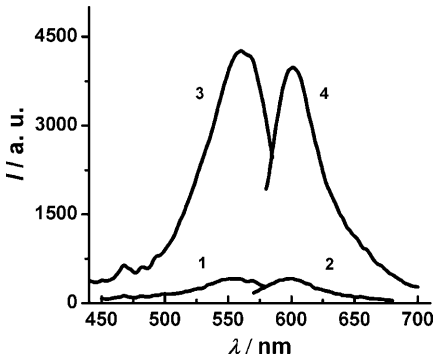

Figure 1. Excitation spectra (lines 1 and 3) and the fluorescence intensity (lines 2 and 4; excitation at 560 nm) of TEMPO–BDP (2.0 μM, 0.10 M DMSO) either with (upper lines) or without (lower lines) 1.0 μM Fe^{2+}/EDTA and 6.0 μM H_2O_2. The spectra were acquired in 10 mM HEPES buffer (pH 7.4). EDTA: ethylenediaminetetraacetate.

The effect of probe concentration: Whether the ·OH could be completely captured or not was determined by the probe concentration, which also affected the accuracy and sensitivity of the proposed method. The results showed that, when the probe concentration was less than 2.0 μM (Figure 2), the

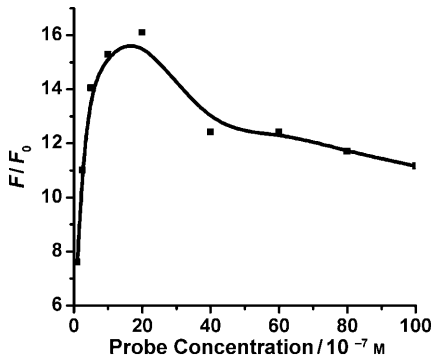

Figure 2. The relationship between the fluorescence intensity and probe concentration. c[Fe^{II}(edta)]: 1.0 μM; [H_2O_2]: 6.0 μM; λ_{ex} = 560 nm, λ_{em} = 601 nm.

F/F_0 (F is the reaction-system fluorescence intensity, and F_0 is the probe fluorescence intensity) value increased with increasing concentrations of the probe. The F/F_0 value was correspondingly stable in the probe-concentration range of 1.0–2.0 μM, whereas it decreased when the concentration was more than 2.0 μM. Therefore, a concentration of 2.0 μM was used in the analytical experiment because the TEMPO–BDP showed the best response to ·OH at this concentration.

Effect of pH value: The probe was insensitive to the pH value as shown in Figure 3, whereas the pH value of the medium did have some effect on the fluorescence intensity of the reaction system. It was clear that the appropriate pH range was from 5.0 to 7.6 (Figure 3). That is to say, TEMPO–BDP works well under physiological conditions (pH 7.4). In order to obtain a lower fluorescence intensity of the reagent blank and a higher signal-to-noise, a pH value of 7.4 in HEPES was employed throughout.

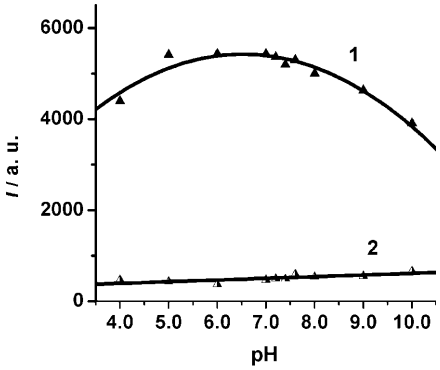

Figure 3. Effect of pH value. Line 1: TEMPO–BDP (2.0 μM, 0.10 M DMSO), Fe^{2+}/EDTA (1.0 μM), H_2O_2 (6.0 μM), 10 mM HEPES buffer; line 2: TEMPO–BDP (2.0 μM, 0.10 M DMSO), no Fe^{2+}/EDTA or H_2O_2, 10 mM HEPES buffer.

The kinetic assay: Tests with different reaction times were carried out. The fluorescence intensity of the reaction system increased markedly with increasing time up to 5 min and leveled off thereafter (Figure 4, line 2). This phenomenon shows that the probe can capture ·OH rapidly, which attests TEMPO–BDP to be a "fast-response" probe. Besides this, the fluorescence intensity of the reaction system did not change after 5 min, which indicated that the reaction product was photostable, whereas the fluorescence intensity of the probe remained basically unchanged for up to 60 min in the absence of ·OH (Figure 4, line 1), which indicated that the probe had good photostability.

Relationship between fluorescence intensity and ·OH concentration: We monitored the changes in the fluorescence spectra of TEMPO–BDP in the presence of different concentrations of ·OH, which are indicated in Figure 5. (·OH was generated quantitively by a Fenton reaction between [Fe^{II}(edta)] (edta: ethylenediaminetetraacetate) and H_2O_2; the [Fe^{II}(edta)] concentrations represented the ·OH concentrations.[37]) As expected, the probe showed weak fluorescence before the addition of ·OH. After the probe had reacted with the ·OH-induced methyl radicals for 10 min, the fluorescence restoration of BDP led rapidly to a significant fluorescence increase (excitation and emission maxima of 560 and 601 nm; see Figure 1). The fluorescence intensity of the probe was enhanced with an increase in the ·OH concentration. Under the optimum experimental conditions, the relative fluorescence intensity was linearly related to the Fe^{2+}/EDTA concentration. The linear regression equations were $\Delta F = 3474.5 + 3385.2$ [Fe^{2+}] (μmol L^{-1}) with a correlation coefficient of 0.9943 in the range of 1.0×10^{-8} to 1.0×10^{-7} M (Figure 6a) and $\Delta F = 3737.6 + 965.1$ [Fe^{2+}] (μmol L^{-1}) with a correlation coefficient of 0.9918 in the range of 1.0×10^{-7} to 1.0×10^{-6} M (Figure 6b), respectively. The detection limit was calculated to be 18 pM, as defined by IUPAC,[38] based on triplicate measurements of the relative standard.

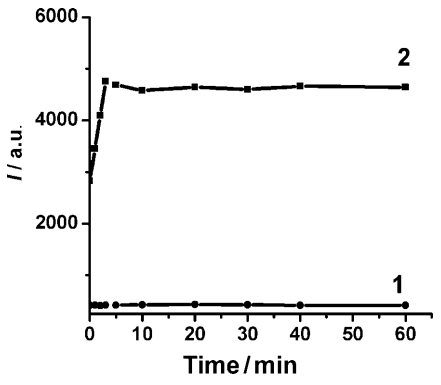

Figure 4. Time course of the TEMPO–BDP reaction measured by spectrofluorometer (λ_{ex} = 560 nm; λ_{em} = 601 nm). The concentration of TEMPO–BDP was 2.0 μM in 10 mM HEPES buffer. Line 1: no ·OH; line 2: 1.0 μM ·OH.

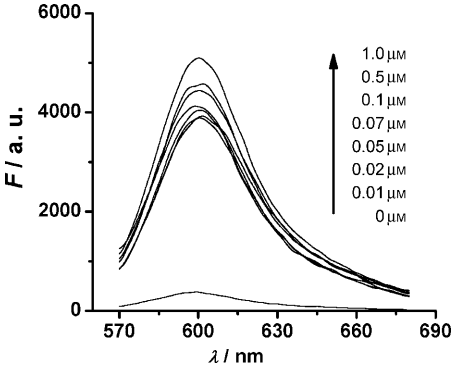

Figure 5. Fluorescence responses of TEMPO–BDP (2.0 μM) toward various concentrations of Fenton reagent ([Fe^{II}(edta)]/H_2O_2, mol/mol = 1:6) as indicated. Final c[Fe^{II}(edta)]: 0–1.0 μM; incubated at 25 °C for 10 min in HEPES (pH 7.4, 10 mM).

Test for probe selectivity: The interference of various bioanalytes, including other ROS and biological antioxidants, was investigated. Figure 7 shows the relative turn-on fluorescence responses of TEMPO–BDP to a panel of biologically

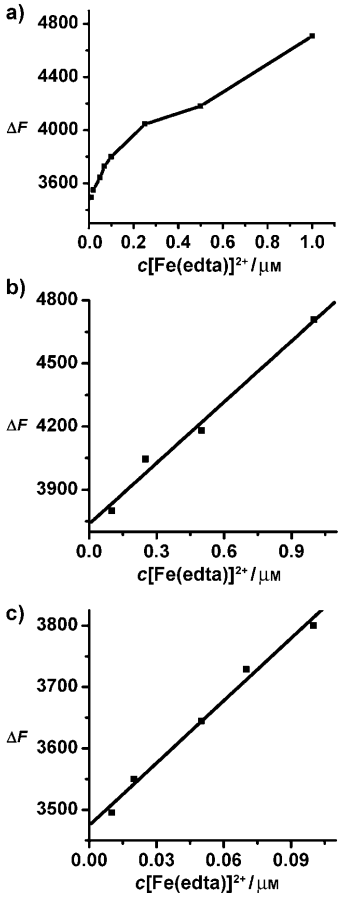

Figure 6. a) Fluorescence responses of TEMPO–BDP (2.0 μM, 0.10 M DMSO) to various concentrations of added $[Fe^{I}(edta)]^{2+}$ and H_2O_2 in 10 mM HEPES buffer (pH 7.4). Linear relationship between relative fluorescence intensity and ·OH concentrations in the range of b) 1.0×10^{-7} to 1.0×10^{-6} M and c) 1.0×10^{-8} to 1.0×10^{-7} M.

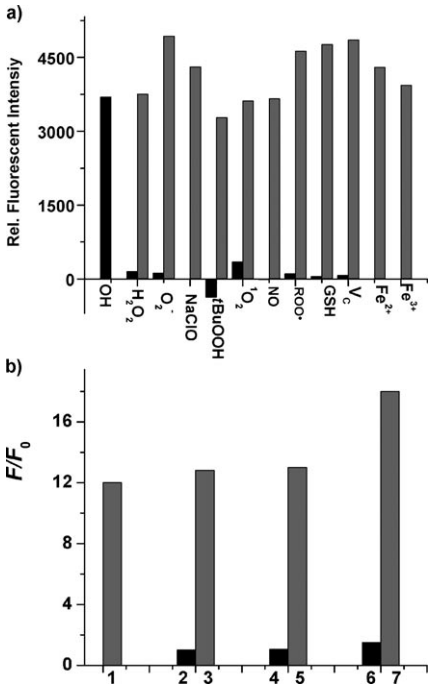

Figure 7. a) Relative fluorescence intensity observed upon reaction of TEMPO–BDP (2.0 μM, 0.10 M DMSO, 10 mM HEPES) with ROS and other biologically relevant compounds. Bars represent relative fluorescence responses to 1.0 μM of each compound. Except for ·OH, two bars are shown for each compound; these represent reactions with 0 μM ·OH (black bar) and 1.0 μM ·OH (gray bar), respectively. b) The probe fluorescence response toward ·OH and $ONOO^-$. Bars represent the final integrated fluorescence response (F) over the initial integrated emission (F_0) with 2.0 μM TEMPO–BDP and 0.10 M DMSO. Conditions: 1) 1.0 μM ·OH; 2) 1.0 μM $ONOO^-$; 3) 1.0 μM $ONOO^-$ and 1.0 μM ·OH; 4) 10 μM $ONOO^-$; 5) 10 μM $ONOO^-$ and 1.0 μM ·OH; 6) 100 μM $ONOO^-$; 7) 100 μM and 1.0 μM ·OH. Data were acquired at 25 °C and pH 7.4 in 10 mM phosphate-buffered saline (PBS) buffer; $\lambda_{ex}=560$, $\lambda_{em}=601$ nm. GSH: glutathione; Vc: ascorbate acid.

relevant substances. It was found that the probe was highly selective for ·OH over other ROS and some biological reductive compounds (Figure 7), like hydrogen peroxide (H_2O_2), superoxide ($O_2^{-\bullet}$), hypochlorite (OCl^-), peroxynitrite ($ONOO^-$), *t*BuOOH, $^1O_2$, NO, ROO·, glutathione, ascorbate acid, and Fe^{2+} and Fe^{3+} ions, owing to its chemospecific nitroxide radical switch. It was an outstanding result that the proposed method was hardly influenced by $ONOO^-$, even when its concentration was ten times that of ·OH (Figure 7b). Therefore, it could be concluded that the probe showed good selectivity for ·OH.

MTT assay: To evaluate cytotoxicity of the probe, we performed an MTT (3-(4,5-dimethylthiazol-2-yl)-2,5-diphenyltetrazolium bromide) assay in RAW264.7 cells with probe concentrations of 10^{-3}, 10^{-4}, 10^{-5}, 10^{-6}, 10^{-7}, and 10^{-8} M. The results showed an IC_{50} value of 69 μM, which clearly demonstrated that the probe had low toxicity to the cultured cell line under experimental conditions at the concentration of 1.0 μM.

Fluorescence confocal microscopy: TEMPO–BDP was tested for its ability to respond toward ·OH in living biosystems by confocal fluorescence microscopy. Probe-loaded mice macrophages displayed strikingly bright fluorescence upon stimulation with phorbol myristate acetate (PMA) for 12 h (Figure 8a and b) in the presence of 0.10 M DMSO. By contrast, macrophages loaded with the probe but with no DMSO and no PMA stimulation (Figure 8c) showed negligible fluorescence. Moreover, macrophages loaded with the probe and 0.10 M DMSO but with no PMA (Figure 8d) and macrophages loaded with the probe and PMA stimulated but with no DMSO (Figure 8e) all gave faint fluorescence. Bright-field measurements indicated that the cells were viable throughout the imaging experiments (Figure 8b). Additionally, the probe showed low cytotoxicity under these experimental conditions by MTT assay. These results demonstrated that the generation of ·OH could be readily imaged by using the probe and that the probe was membrane permeable and had low cytotoxicity to cells. The probe could respond to the changes of ·OH concentrations in living cells with high sensitivity.

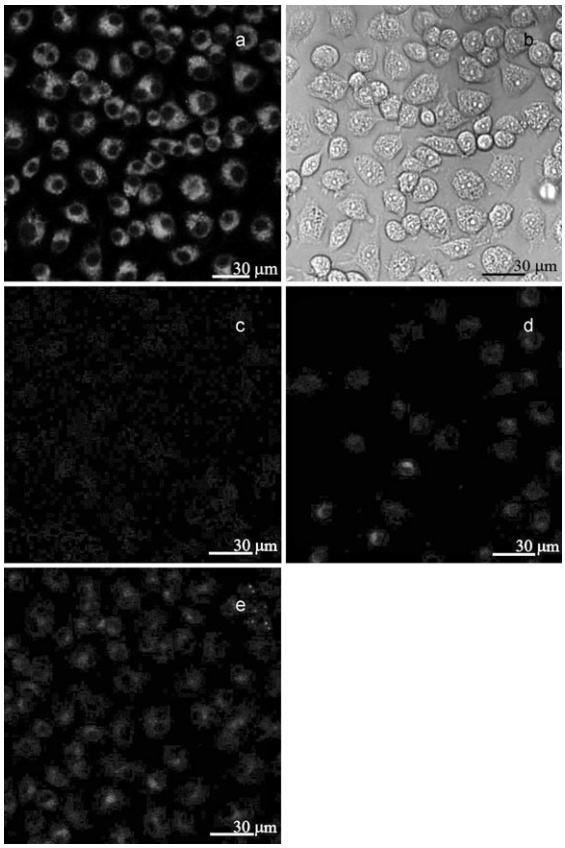

Figure 8. Confocal fluorescence images of living mice macrophages (RAW264.7) under different conditions with TEMPO–BDP. Mice macrophages were incubated with 1.0 μM TEMPO–BDP for 15 min at 37 °C and then imaged. a) Imaged with TEMPO-BDP upon stimulation with PMA for 12 h in 0.10 M DMSO (with a 30 μm scale bar). b) Brightfield image under the same conditions as (a). c) Imaged with TEMPO-BDP but not stimulated and with no DMSO. d) Imaged with TEMPO-BDP and 0.10 M DMSO but not stimulated. e) Imaged with TEMPO-BDP and stimulated with PMA for 12 h but with no DMSO.

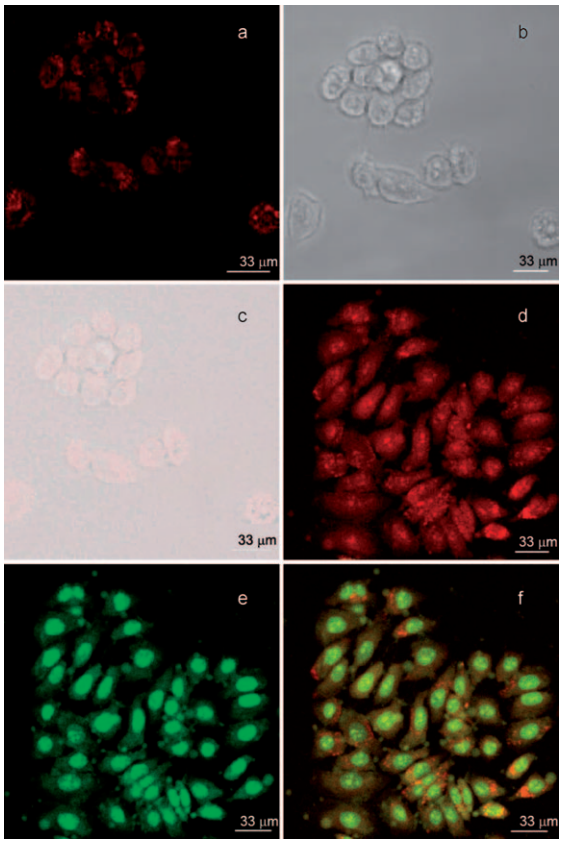

Figure 9. Imaging of normal human liver (HL-7702) cells and human hepatoma (HepG2) cells. a) Probe-loaded HL-7702 fluorescence image; b) brightfield image; c) overlay of (a) and (b). d) Fluorescence image of HepG2 cells loaded with the probe; e) fluorescence image of HepG2 cells loaded with Acridine Orange; f) overlay of (d) and (e). HL-7702 and HepG2 cells were separately incubated in 1.0 μM TEMPO–BDP and 0.10 M DMSO for 15 min and then were rinsed 3 times with PBS.

Fluorescence imaging in normal human liver (HL-7702) and human hepatoma (HepG2) cells: To verify the feasibility of the probe, fluorescence image experiments were carried out in other biological models. Extensive studies demonstrate that tumor occurrence is related with reactive oxygen species.[39] Therefore, we selected normal human liver (HL-7702) cells and human hepatoma (HepG2) cells to investigate whether there were fluorescence-brightness distinctions between normal cells and tumor cells (Figure 9). Images revealed that HepG2 cells (Figure 9d) showed stronger fluorescence than HL7702 cells (Figure 9a). These results indicated that the $^{\bullet}OH$ concentration in HepG2 cells should be higher than that in HL7702 cells, which foreshadows broad application prospects of the probe in biological systems. Additionally, the probe showed low cytotoxicity under these experimental conditions because the cell morphology was scatheless, as determined by comparison with the image of cells dyed with Acridine Orange, which is used to intuitively evaluate the living-cell activity (Figure 9e and f).

Conclusions

We designed and synthesized a new nonredox fluorescent probe to realize the imaging of $^{\bullet}OH$ in living cells. This probe rapidly responded to $^{\bullet}OH$, with a detection limit of 18 pM. Moreover, the probe was quite photostable and less sensitive to pH changes. Other ROS and relevant intracellular components did not interfere. Most importantly, the major problem of $ONOO^-$ interference was efficiently avoided. Better than the currently available probes, this probe could penetrate into intact cell membranes to selectively detect intracellular $^{\bullet}OH$ without causing cellular damage. We believe that this probe will be broadly applicable to the quantitative detection of $^{\bullet}OH$ in biological systems.

Experimental Section

Chemicals: Xanthine (X; 1 mM) in 10 mM NaOH solution, xanthine oxidase (XO; 5 U mL^{-1}), 3-(2-hydroxy-1-(1-methylethyl)-2-nitrosohydrazino)-1-propanamine (NOC-5), 2,2′-azobis(2-amidinopropane) dihydro-

chloride (AAPH), ascorbic acid, L-glutathione, DMSO (99.9%), and PMA were all purchased from Sigma. All chemicals used were of analytical-reagent grade. Purification water used throughout was from a Sartorius ultrapurification system. 4-Hydroxy-2,2,6,6-tetramethyl-1-piperidinoxyl (4-hydroxy-TEMPO) was also purchased from Sigma.

Instruments: Fluorometric traces were obtained with an Edinburgh FLS920 spectrofluorimeter (Edinburgh Instruments Ltd, England) with a Xenon lamp and 1.0 cm quartz cells; excitation and emission band passes were both set to 2 nm. ^{1}H NMR spectra were recorded on a Bruker Avance 300. Elemental analysis was performed on Perkin–Elmer Series II CHNS/O analyzer.

Synthesis of 2-[4′-(2,2,6,6-tetramethyl-1-piperidinoxyl)-oxyl]-4,4-difluoro-1,3,5,7-tetraphenyl-4-bora-3*a*,4*a*-diaza-*s*-indacene (TEMPO–BDP): 8-Chloromethyl-4,4-difluoro-1,3,5,7-tetraphenyl-4-bora-3*a*,4*a*-diaza-*s*-indacene (BDP) was prepared by established methods.[40] A slurry of NaH (0.3 g, 11.6 mmol, 80% in mineral oil, washed with hexane) was added into a solution of 4-hydroxy-TEMPO (1.0 g, 5.8 mmol) dissolved in *N*,*N*-dimethylformamide (DMF; 30 mL), and the mixture was stirred at RT under an Ar atmosphere. After 2 h, excess BDP in DMF (50 mL) was added with stirring under an Ar atmosphere. The reaction was completed after 22 h at RT. The solvent was removed under vacuum, and then the residue was chromatographically separated on a silica gel column by eluting with CH_2Cl_2/petroleum ether (5:2) to give the product as a fuchsia solid (0.28 g, 58%); m.p. 220–221 °C; ^{1}H NMR (300 MHz, $CDCl_3$, 25 °C, tetramethylsilane (TMS)): $\delta = 7.13$–7.80 (20H), 4.00 (2H), 1.12 (12H), 1.39, 1.63 (4H), 2.79 ppm (1H); ^{13}C NMR (75 MHz, $CDCl_3$, 25 °C, TMS): $\delta = 155.6$, 146.0, 136.9, 132.6, 129.6, 129.2, 128.8, 128.7, 128.4, 128.0, 127.9, 127.7, 124.0, 123.8, 122.7, 119.0, 98.5, 94.2, 59.5, 53.3, 39.3, 24.4, 22.6 ppm; GC–MS (API-ES): *m*/*z* calcd: 679.33; found: 678.29 $[M]^+$; elemental analysis: calcd for $C_{43}H_{41}BF_2N_3O_2^{\bullet}$: C 75.88, H 6.07, N 6.17; found: C 75.48, H 6.01, N 6.09. The synthetic route is illustrated in Scheme 2.

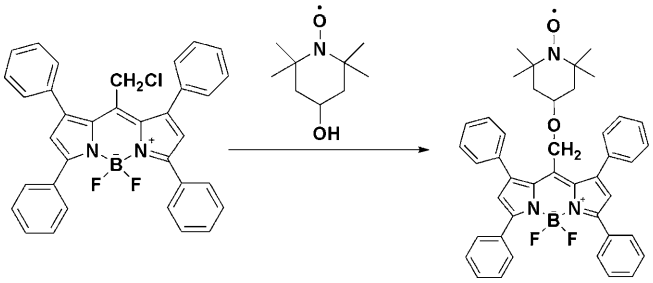

Scheme 2. The synthetic route for TEMPO–BDP.

Fluorescence spectra of excitation and emission: Purified TEMPO–BDP was first dissolved in a small volume of DMSO and then diluted into the standard buffer. The spectral properties of TEMPO–BDP were tested by its reaction with hydroxyl radicals under simulated physiological conditions (pH 7.4, HEPES buffer, final concentration 10 mM). Various concentrations of Fe^{2+}/EDTA and H_2O_2, were mixed to produce the hydroxyl radicals. After 15 min, DMSO, TEMPO–BDP (final concentration of 2.0 μM), and HEPES buffer were added in turn. The mixture was then diluted to volume with ultrapure water and left for 10 min before determination. After that, the fluorescence intensity was measured at $\lambda_{ex/em} = 560/601$ nm against a reagent blank. The excitation and emission slits were both set to 2 nm. The quantum yields of fluorescence were determined by using rhodamine B ($\phi = 0.65$, 10^{-6} M in ethanol) as a standard substance against a secondary standard.[41]

Interference assay: $^1O_2$ was generated by the reaction of H_2O_2 with NaClO, and $O_2^{-\bullet}$ was created by the enzymatic reaction of xanthine/xanthine oxidase (XA/XO; 6.0 μM/3 mU) at 25 °C for 5 min. NO was produced by NOC-5. ROO• was generated by AAPH. The concentrations of H_2O_2, NaClO, *t*BuOOH, NOC-5, GSH, and Vc were all 1.0 μM. $ONOO^-$ was prepared by KNO_2 and H_2O_2 in HCl at 0 °C as previously reported[42] and was frozen at less than −18 °C. Peroxynitrite concentrations were measured spectrophotometrically in aliquots thawed immediately before use in the experiments, by using an extinction coefficient of $1670\,M^{-1}cm^{-1}$ at 302 nm in 0.10 M NaOH. All interference experiments were carried out with the relevant compounds alone and in the presence of •OH, to observe the probe response to the above substances.

Cell culture: Primary cultured macrophages (RAW264.7, purchased from the Committee on Type Culture Collection of the Chinese Academy of Sciences) were grown in a cell-culture flask (1×10^6 cell mL^{-1}) in high-glucose Dulbecco's modified Eagle's medium supplemented with 10% fetal bovine serum (FBS), 1% penicillin, and 1% streptomycin. Cultures were maintained at 37 °C under a humidified atmosphere containing 5% CO_2 until further analysis. Normal human liver (HL-7702) cells and hepatoma (HepG2) cells were cultured continuously in Rosewell Park Memorial Institute 1640 medium supplemented with 10% FBS, 1% penicillin, and 1% streptomycin. Cultures were maintained at 37 °C under a humidified atmosphere containing 5% CO_2.

Confocal fluorescence image assay: A set of cells were stimulated with PMA (2 ng ml^{-1}; a stimulator of cell respiratory burst to give rise to ROS) at 37 °C.[43] Cells were washed three times with PBS buffer before imaging. The images were taken by using an LTE confocal laser scanning microscope (Germany Leica Co., Ltd) with an objective lens (×40). All background parameters (the laser intensity, exposure time, objective lens) were stationary when the different fluorescence images were captured. The excitation wavelengths of TEMPO-BDP and Acridine Orange were 532 and 488 nm, respectively.

MTT assay: Macrophages (10^6 cell mL^{-1}) were dispersed within replicate 96-well microtiter plates to a total volume of 200 μL well^{-1}. Plates were maintained at 37 °C in a 5% CO_2/95% air incubator for 5 hours. Macrophages were then incubated for 24 hours with different probe concentrations of 10^{-3}, 10^{-4}, 10^{-5}, 10^{-6}, 10^{-7}, and 10^{-8} M, respectively. MTT (Sigma) solution (5 mg mL^{-1} in PBS) was then added to each well. After 4 h, the remaining MTT solution was removed and DMSO (150 μL) was added to each well to dissolve the formazan crystals. The absorbance was measured at 490 nm in a TRITURUS microplate reader. The calculation of IC_{50} values was done according to the method of Huber and Koella.[44]

Acknowledgements

This work was supported by the National Basic Research Program of China (973 Program, 2007CB936000), the National Natural Science Funds for Distinguished Young Scholar (No. 20725518), the Major Program of the National Natural Science Foundation of China (no. 90713019), the Science and Technology Development Programs of Shandong Province of China (no. 2008GG30003012), and the Research Foundation for the Doctoral Program of Ministry of Education (no. 20060445002).

[1] H. Wiseman, B. Halliwell, *Biochem. J.* **1996**, *313*, 17–29.
[2] J. M. McCord, *Science* **1974**, *185*, 529–531.
[3] K. Dobashi, B. Ghosh, J. K. Orak, I. Singh, *Biochem.* **2000**, *205*, 1–11.
[4] M. Nishida, Y. Maruyama, R. Tanaka, K. Kontani, T. Nagao, T. Hoshi, *Nature* **2000**, *408*, 492–495.
[5] D. A. Benoît, B. T. Michel, *Nat. Rev. Mol. Cell Biol.* **2007**, *8*, 813–824.
[6] K. Ishikawa, K. Takenaga, M. Akimoto, N. Koshikawa, A. Yamaguchi, H. Imanishi, K. Nakada, Y. Honma, J. Hayashi, *Science* **2008**, *320*, 661–664.
[7] T. Az-ma, N. Saeki, O. B. Jyuge, *J. Pharm.* **1999**, *126*, 1462–1470.
[8] A. Gomes, E. Fernandes, J. L. F. C. Lima, *J. Biochem. Biophys. Methods* **2005**, *65*, 45–80.
[9] B. Halliwell, M. B. Whiteman, *J. Pharmacol.* **2004**, *142*, 231–255.
[10] X. F. Yang, X. Q. Guo, *Analyst* **2001**, *126*, 1800–1804.
[11] B. Li, P. L. Gutierrez, N. V. Blough, *Anal. Chem.* **1997**, *69*, 4295–4302.

[12] B. Tang, L. Zhang, Y. Geng, *Talanta* **2005**, *65*, 769–775.
[13] H. Ischiropoulos, A. Gow, S. R. Thom, N. W. Kooy, J. A. Royall, J. P. Crow, *Methods Enzymol.* **1999**, *301*, 367–373.
[14] C. P. Lebel, H. Ischiropoulos, S. C. Bondy, *Chem. Res. Toxicol.* **1992**, *5*, 227–231.
[15] T. Ohashi, A. Mizutani, A. Murakami, S. Kojo, T. Ishii, S. Taketani, *FEBS Lett.* **2002**, *511*, 21–27.
[16] P. Wardman, M. J. Burkitt, K. B. Patel, A. Lawrence, C. M. Jones, S. A. Everett, B. J. Vojnovic, *J. Fluoresc.* **2002**, *12*, 65–68.
[17] O. Myhre, J. M. Andersen, H. Aarnes, F. Fonnum, *Biochem. Pharmacol.* **2003**, *65*, 1575–1582.
[18] K. I. Setsukinai, Y. Urano, K. Kakinuma, H. J. Majima, T. Nagano, *J. Biol. Chem.* **2003**, *278*, 3170–3175.
[19] S. Pou, Y. I. Huang, A. Bhan, V. S. Bhadti, R. S. Hosmane, S. Y. Wu, G. L. Cao, G. M. Rosen, *Anal. Biochem.* **1993**, *212*, 85–90.
[20] S. E. Buxser, G. Sawada, T. J. Raub, *Methods Enzymol.* **1999**, *300*, 256–275.
[21] Y. Manevich, K. D. Held, J. E. Biaglow, *Radiat. Res.* **1997**, *148*, 580–591.
[22] G. M. Makrigiorgos, J. Baranowska-Kortylewicz, E. Bump, S. K. Sahu, R. M. Berman, A. I. Kassis, *Int. J. Radiat. Biol.* **1993**, *63*, 445–458.
[23] C. Tai, X. Gu, H. Zou, Q. Guo, *Talanta* **2002**, *58*, 661–667.
[24] B. Tang, N. Zhang, Z. Chen, K. Xu, L. Zhuo, L. An, G. Yang, *Chem. Eur. J.* **2008**, *14*, 522–528.
[25] N. V. Blough, D. J. Simpson, *J. Am. Chem. Soc.* **1988**, *110*, 1915–1917.
[26] M. K. Eberhardt, R. Colina, *J. Org. Chem.* **1988**, *53*, 1071–1074.
[27] E. Vos de Wal, J. A. Pardoen, J. A. van Koeveringe, J. Lugtenburg, *Recl. Trav. Chim. Pays-Bas.* **1977**, *96*, 306–309.
[28] J. Karolin, L. B. A. Johansson, L. Strandberg, T. Ny, *J. Am. Chem. Soc.* **1994**, *116*, 7801–7806.
[29] S. A. Green, D. J. Simpson, G. Zhou, P. S. Ho, N. V. Blough, *J. Am. Chem. Soc.* **1990**, *112*, 7337–7346.
[30] J. A. Green, L. A. Singer, J. H. Parks, *J. Chem. Phys.* **1973**, *58*, 2690–2695.
[31] P. E. Benville, C. E. Smith, W. E. Shanks, *Toxicol. Appl. Pharmacol.* **1968**, *12*, 156–178.
[32] *Toxicology of DMSO in animals* (Eds.: M. M. Mason, S. W. Jacob, E. E. Rosen, D. C. Wood), Dekker, New York, **1971**, p. 113.
[33] R. R. Maurer, *The Freezing of Mammalian Embryos*, Elsevier, Amsterdam, **1977**, p. 116.
[34] I. Wilmut, L. E. A. Rowson, *Vet. Rec.* **1973**, *92*, 686.
[35] S. M. Willadsen, *The Freezing of Mammalian Embryos*, Elsevier, Amsterdam, **1977**, p. 175.
[36] M. J. Ashwood-Smith, N. Y. Ann, *Acad. Sci.* **1975**, 243–246.
[37] B. Halliwell, J. M. C. Gutteridge, *Arch. Biochem. Biophys.* **1986**, *246*, 501–514.
[38] H. M. N. H. Irving, H. Freiser, T. S. West, *IUPAC Compendium of Analytical Nomenclature Definitive Rules*, Pergamon Press, Oxford, **1978**.
[39] J. M. McCord, *Science* **1974**, *185*, 529–531.
[40] L. Zeng, E. W. Miller, A. Pralle, E. Y. Isacoff, C. J. Chang, *J. Am. Chem. Soc.* **2006**, *128*, 10–11.
[41] R. A. Velapoldi, H. H. Tonnesen, *J. Fluoresc.* **2004**, *14*, 465–472.
[42] J. W. Reed, H. H. Ho, W. L. Jolly, *J. Am. Chem. Soc.* **1974**, *96*, 1248–1249.
[43] Y. Okimotoa, A. Watanabea, E. Nikia, T. Yamashitab, N. Noguchia, *FEBS Lett.* **2000**, *474*, 137–140.
[44] W. Huber, J. C. Koella, *Acta Trop.* **1993**, *55*, 257–261.

Received: June 4, 2009
Revised: October 8, 2009
Published online: December 11, 2009

